

Development and Evaluation of an Optimal Human Single-Chain Variable Fragment-Derived BCMA-Targeted CAR T Cell Vector

Eric L. Smith,^{1,2} Mette Staehr,^{1,7} Reed Masakayan,^{1,7} Ishan J. Tatake,¹ Terence J. Purdon,¹ Xiuyan Wang,³ Pei Wang,⁴ Hong Liu,⁴ Yiyang Xu,⁴ Sarah C. Garrett-Thomson,⁵ Steven C. Almo,⁵ Isabelle Riviere,³ Cheng Liu,⁴ and Renier J. Brentjens^{1,6}

¹Cellular Therapeutics Center, Memorial Sloan Kettering Cancer Center, New York, NY, USA; ²Myeloma Service, Memorial Sloan Kettering Cancer Center, New York, NY, USA; ³Cell Therapy and Cell Engineering Facility, Memorial Sloan Kettering Cancer Center, New York, NY, USA; ⁴Eureka Therapeutics, Emeryville, CA, USA; ⁵Department of Biochemistry, Albert Einstein College of Medicine, Bronx, NY, USA; ⁶Leukemia Service, Memorial Sloan Kettering Cancer Center, New York, NY, USA

B cell maturation antigen (BCMA) has recently been identified as an important multiple myeloma (MM)-specific target for chimeric antigen receptor (CAR) T cell therapy. In CAR T cell therapy targeting CD19 for lymphoma, host immune anti-murine CAR responses limited the efficacy of repeat dosing and possibly long-term persistence. This clinically relevant concern can be addressed by generating a CAR incorporating a human single-chain variable fragment (scFv). We screened a human B cell-derived scFv phage display library and identified a panel of BCMA-specific clones from which human CARs were engineered. Despite a narrow range of affinity for BCMA, dramatic differences in CAR T cell expansion were observed between unique scFvs in a repeat antigen stimulation assay. These results were confirmed by screening in a MM xenograft model, where only the top performing CARs from the repeat antigen stimulation assay eradicated disease and prolonged survival. The results of this screening identified a highly effective CAR T cell therapy with properties, including rapid *in vivo* expansion (>10,000-fold, day 6), eradication of large tumor burden, and durable protection to tumor re-challenge. We generated a bicistronic construct including a second-generation CAR and a truncated-epithelial growth factor receptor marker. CAR T cell vectors stemming from this work are under clinical investigation.

INTRODUCTION

Chimeric antigen receptor (CAR) T cell therapy has demonstrated dramatic efficacy in patients with relapsed or refractory CD19⁺ malignancies such as adult^{1–3} and pediatric B cell acute lymphocytic leukemia (ALL),⁴ and non-Hodgkin's lymphoma (NHL).^{5–7} However, to extend the potential benefits of CAR T cell therapy beyond CD19⁺ malignancies, CARs incorporating single-chain variable fragments (scFvs) targeting additional antigens must be developed. B cell maturation antigen (BCMA; *TNFRSF17*), a differentiated B cell/plasma cell specific trans-membrane receptor, has been recognized as an ideal CAR T cell target for multiple myeloma (MM) given its near-uniform

and ubiquitous expression on MM cells, role in MM cell growth, and lack of expression on other essential cell types.^{8–12}

A CAR typically consists of an extracellular scFv, a spacer/hinge region, a transmembrane domain, and intracellular signaling domain(s). Clinical CAR T cell therapy constructs have primarily utilized a second-generation CAR, where the signaling domains are derived from the T cell receptor CD3-zeta chain, providing activation (signal 1), and a signaling domain from either CD28 or 4-1BB, providing co-stimulation (signal 2). In addition to intracellular signaling domains, the extracellular components can have an impact on the properties CARs impart to gene-modified T cells. Importantly, characteristics of the scFv, such as the affinity of an scFv,^{13–15} the location of the epitope the scFv recognizes,^{15,16} and likely many other attributes of the scFv all can contribute to the efficacy of CAR T cell therapy.

An additional, less appreciated, property of the scFv to consider in CAR design is its immunogenicity. Until recently, most CARs contained an scFv derived from murine antibodies. However, patient anti-murine immunity can be a clinically relevant limitation to CAR T cell therapy mediated by incorporation of a murine scFv. For example, in a trial of anti-CD19(FMC63)/4-1BBz CAR T cell therapy for NHL, several patients relapsed with CD19⁺ disease and were treated with a second dose of autologous CAR T cells. In all five such patients, some of whom were treated with a 10-fold higher second dose, unlike after the initial infusion, there was not an expansion of CAR T cells in the peripheral blood, nor was there any appreciable anti-lymphoma activity. Researchers at the Fred Hutchinson Cancer Research Center (FHRC) identified host cellular immunity

Received 7 February 2018; accepted 23 March 2018;
<https://doi.org/10.1016/j.ymthe.2018.03.016>

⁷These authors contributed equally to this work.

Correspondence: Renier J. Brentjens, MD, PhD, Cellular Therapeutics Center, Memorial Sloan Kettering Cancer Center, New York, NY, USA.

E-mail: brentj@mskcc.org



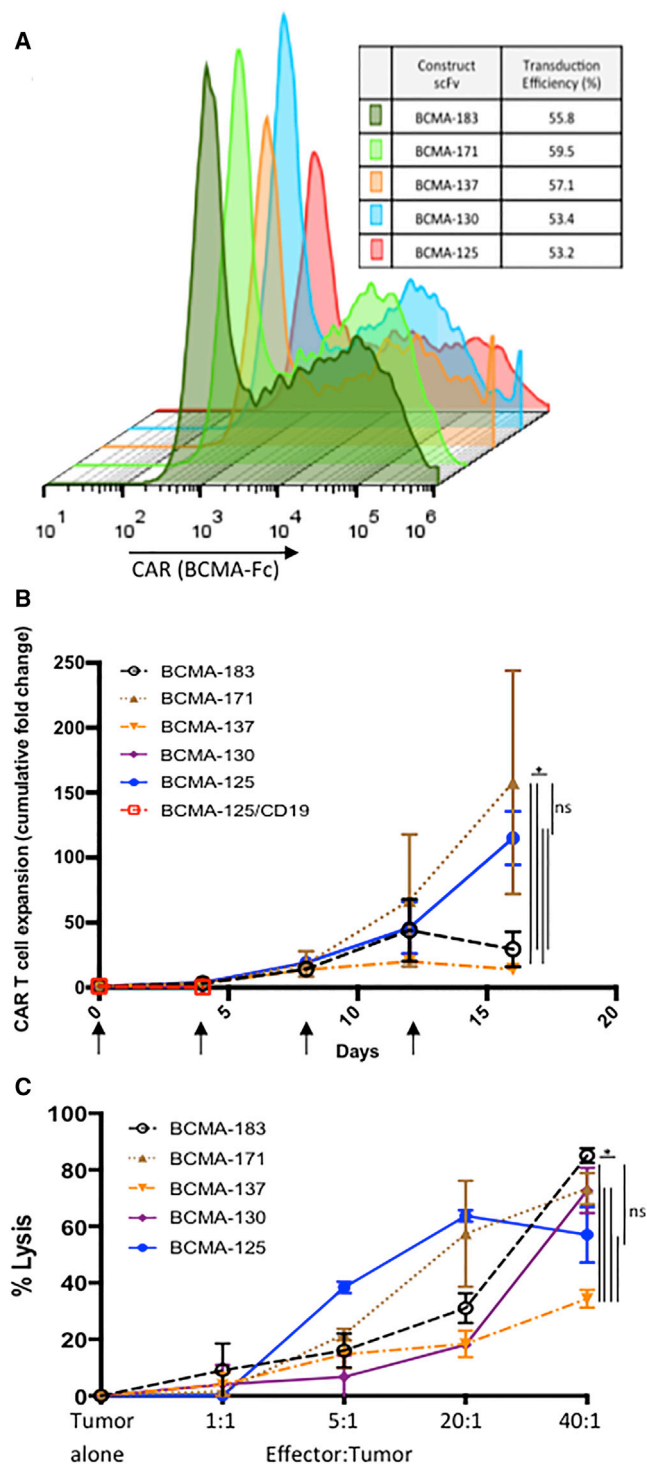


Figure 1. Superior Expansion of BCMA(171) and BCMA(125) scFv Containing CAR T Cells Demonstrated by Repeat Antigen Stimulation Assay

(A) Retroviral transduction efficiency; cell surface staining of human T cells is consistent regardless of scFv. Results from representative single donor. (B) Repeat antigen stimulation assay; CAR T cells containing scFvs indicated (CD28

specific to peptides from the FMC63 murine scFv in 80% of these patients.⁷ A separate trial of carbonic anhydrase 9 (CAIX)-targeted CAR T cell therapy for renal cell carcinoma also documented patient anti-murine scFv immune responses.¹⁷ Patient anti-CAR immunity can potentially be averted by designing a fully human CAR, incorporating a human B cell-derived scFv.

Herein, we report the development of the first human scFv-derived CAR targeting BCMA. We describe the strategies and rationale used to differentiate between CARs containing unique human scFvs and identify scFv-mediated differences in expansion after repeat antigen stimulation as a particularly informative assay in optimizing CAR design. Additionally, we characterize the kinetics of *in vivo* expansion and accumulation of T cells genetically modified with our lead CAR. Highly active human BCMA-targeted CAR constructs stemming from this work are currently under clinical evaluation.

RESULTS

Identification of Human Anti-BCMA scFvs for Incorporation into CAR Vectors

We screened a human B cell-derived scFv phage display library (Figure S1) containing 6×10^{10} scFvs with recombinant human BCMA extracellular domain-immunoglobulin G1 (IgG1) Fc fusion (BCMA-Fc) protein to identify BCMA-specific human scFvs. After DNA sequencing, 57 unique and diverse BCMA-specific clones were identified containing light- and heavy-chain CDRs, each covering six subfamilies with HCDR3 length ranging from 5 to 18 amino acids. The binding specificity of the unique clones against full-length human BCMA expressing NIH 3T3 murine fibroblast artificial antigen-presenting cells (BCMA-aAPCs) was confirmed by flow cytometric analysis. 17 clones were further confirmed to bind to human MM cell lines by flow cytometry, and a subset of these scFvs were directly cloned into second-generation CAR vectors in a retroviral plasmid.

Flow cytometric analysis after staining with BCMA-Fc confirmed CAR expression on the cell surface of donor T cells; we consistently achieve similar retroviral transduction efficiencies (50%–60%) across scFvs investigated (Figure 1A). The majority of BCMA-targeted scFvs investigated had similar, single-digit nanomolar affinity for BCMA (Table S1).

co-stimulatory domain) were placed on BCMA-aAPC or CD19-aAPC monolayers. Every 4 days, CAR T cells are counted, and the same number of CAR⁺ T cells are re-plated on a new aAPC monolayer (arrows). CARs containing human anti-BCMA scFvs 171 and 125 convey superior expansion when plated on BCMA-aAPCs; mean \pm SEM; three independent experiments/donors; BCMA(125) CAR T cells, plated on CD19 aAPCs do exhibit expansion at day 4. (C) Cytotoxicity analysis; CAR⁺ T cells transduced with the same constructs as 1b are co-cultured at increasing E:T ratios with OPM2 human myeloma cell line. All scFvs lyse OPM2 cells in a dose-dependent manner. CAR T cells incorporating scFvs 183, 171, 130, and 125 are superior to 137; mean \pm SEM; representative experiment in triplicate (* $p < 0.005$, two-way ANOVA). aAPC, NIH 3T3 artificial antigen presenting cell.

CAR T Cell Expansion after Repeat Antigen Stimulation Distinguishes between scFv Clones

As in B cell ALL,¹ in CAR T cell clinical trials of MM,¹⁰ CAR T cell expansion in patients appears to correlate with clinical efficacy. *In vivo*, CAR T cells are required to expand in the setting of continuous exposure to target antigen in order to eradicate large tumor burdens. For this reason, we sought to assess the *in vitro* expansion potential of CAR T cells over multiple cycles of antigen stimulation. This repeat antigen stimulation assay revealed substantial differences in the expansion between novel scFvs incorporated into our CD28 containing CAR constructs, identifying scFv clones 125 and 171 [BCMA(125), and BCMA(171), respectively] as superior expanders compared to those incorporating other scFvs. For example, BCMA(171) and BCMA(125) CAR T cells uniquely continued to expand after four stimulations and expanded between a mean of 115- and 158-fold, respectively, across experiments using three independent donors ($p < 0.005$ compared to any other CAR). None of the other scFvs studies continued to expand past the fourth stimulation, a group where peak expansion was limited to between 2- and 30-fold (Figure 1B).

Comparing cytotoxicity between these same CARs containing unique scFvs does not yield the same magnitude of differences as the repeat antigen stimulation assay. To analyze cytotoxicity, we quantified ATP-dependent bioluminescence of an OPM2 MM cell line target transduced with firefly luciferase (ffLuc) 4 hr after co-culture with CAR T cells.¹⁸ Cytotoxicity against OPM2-ffLuc cells demonstrate that CAR T cells incorporating any of the anti-BCMA scFv studies lyse MM cell lines in a dose-dependent manner. However, it could not differentiate between the majority of CARs, with BCMA(183), BCMA(171), BCMA(130), and BCMA(125) all generating statistically equivalent cytotoxicity; only BCMA(137) was inferior to the rest ($p < 0.005$; Figure 1C).

In Vivo Assessment of Human Anti-BCMA CARs Confirms Results of *In Vitro* Repeat Antigen Stimulation Assay in Distinguishing between Anti-BCMA scFvs

NOD *scid* gamma (NSG) mice were engrafted with the bone marrow tropic human MM cell line OPM2.¹⁹ A large burden of disease was permitted to establish over 21 days after tail-vein injection of OPM2-ffLuc cells before treatment with a single injection of donor T cells modified with the same CARs as above. Confirming the predictive value of the repeat antigen stimulation assay, only BCMA(125) and BCMA(171) containing CAR T cells improved the survival of mice, while, despite *in vitro* anti-tumor activity, CAR T cells containing scFvs 183, 137, and 130 exhibited no meaningful anti-MM efficacy in this high tumor burden model of MM ($p < 0.001$; Figure 2A). Bioluminescent imaging (BLI) demonstrated that eradication of OPM2-ffLuc cells was similarly limited to mice treated with BCMA(125) and BCMA(171) CAR T cells (Figure 2B). While both scFvs were equivalent over a variety of assays, we selected BCMA(171) to further characterize and evaluate more closely for clinical translation.

BCMA(171) CAR T Cells Can Provide Long-Term Protection against MM Re-challenge

The ability of human anti-BCMA CARs incorporating clone 171 with either CD28 or 4-1BB co-stimulatory domains to provide long-lasting protection against endogenous BCMA expressing MM cell line re-challenge was assessed by a second injection of OPM2-ffLuc cells in long-term surviving mice, 98 days after the initial injection. NSG mice were first injected (day 0) with OPM2-ffLuc cells. They were treated 4 days later with either BCMA(171)/4-1BBz, BCMA(171)/CD28z, or control CD19(SJ25C1)/CD28z CAR T cells. Both increased survival ($p < 0.001$, Figure 3A) and eradicated tumor (Figure 3B). In contrast to the high disease burden model (Figure 2), in this model we saw a high incidence of xenogeneic graft-versus-host disease (GvHD), requiring euthanasia. It is possible that in eradicating a high disease burden, CAR T cells exhausted their proliferative potential and were less able to cause GvHD, a previously reported phenomena.²⁰ Long-term surviving mice, at day 98, were then re-challenged with a second injection of OPM2-ffLuc cells. Mice were not re-treated with another dose of CAR T cells; however, these long-term surviving mice were protected from tumor re-challenge, presumably by their initial CAR T cell treatment 94 days earlier, as they, unlike CAR T cell-naive control mice injected at the same time, continued to survive another 80 days ($p < 0.001$; Figure 3C) without the re-establishment of tumor (Figure 3D).

BCMA(171) CAR T Cells Rapidly Home to, Accumulate, and Eradicate Tumor in an Established MM Model

We designed a bicistronic retroviral vector including a second generation BCMA(171)/4-1BBz CAR and exterior Gaussia luciferase (extGLuc) to monitor the distribution and expansion of CAR T cells *in vivo* over time. ExtGLuc generates bioluminescence in the presence of its substrate, coelenterazine (CTZ), but not in the presence of luciferin, the substrate of ffLuc. CTZ has a rapid half-life *in vivo*, and thus, extGLuc and ffLuc can be sequentially imaged in the same imaging session.¹⁹ We demonstrate extGLuc/CAR T cell accumulation at the site of OPM2-ffLuc tumors within 24 hr of their injection. ExtGLuc/CAR T cell accumulation expands rapidly at this site over the first 6 days after injection, eradicating the MM xenograft in this time frame. After the clearance of antigen, CAR T cells then contract (Figure 4A). Peak BLI at the site of MM in the area of the femur occurred on day 6 after CAR T cell injection; a mean increase in BLI signal of 14,610-fold occurred between imaging at 24 hr to peak signal ($n = 6$; range 9,593–19,993 fold increase). Mean BLI signal of extGLuc BCMA(171)-targeted CAR T cells reached a peak of 1.5×10^9 photons/s, compared to extGLuc CD19(SJ25C1)-targeted CAR T cells, where mean peak BLI signal was 5.3×10^5 photons/s ($p < 0.0001$; Figures 4B and 4C).

Human scFvs Are Specific for BCMA

BCMA is a member of the tumor necrosis factor receptor superfamily (TNFRSF) with a known role in differentiated B cell/plasma cell/MM cell biology,¹² and several studies have found its expression to be limited to these cell types.^{8,9} However, validation of target specificity is essential for novel scFvs with potential clinical application. An

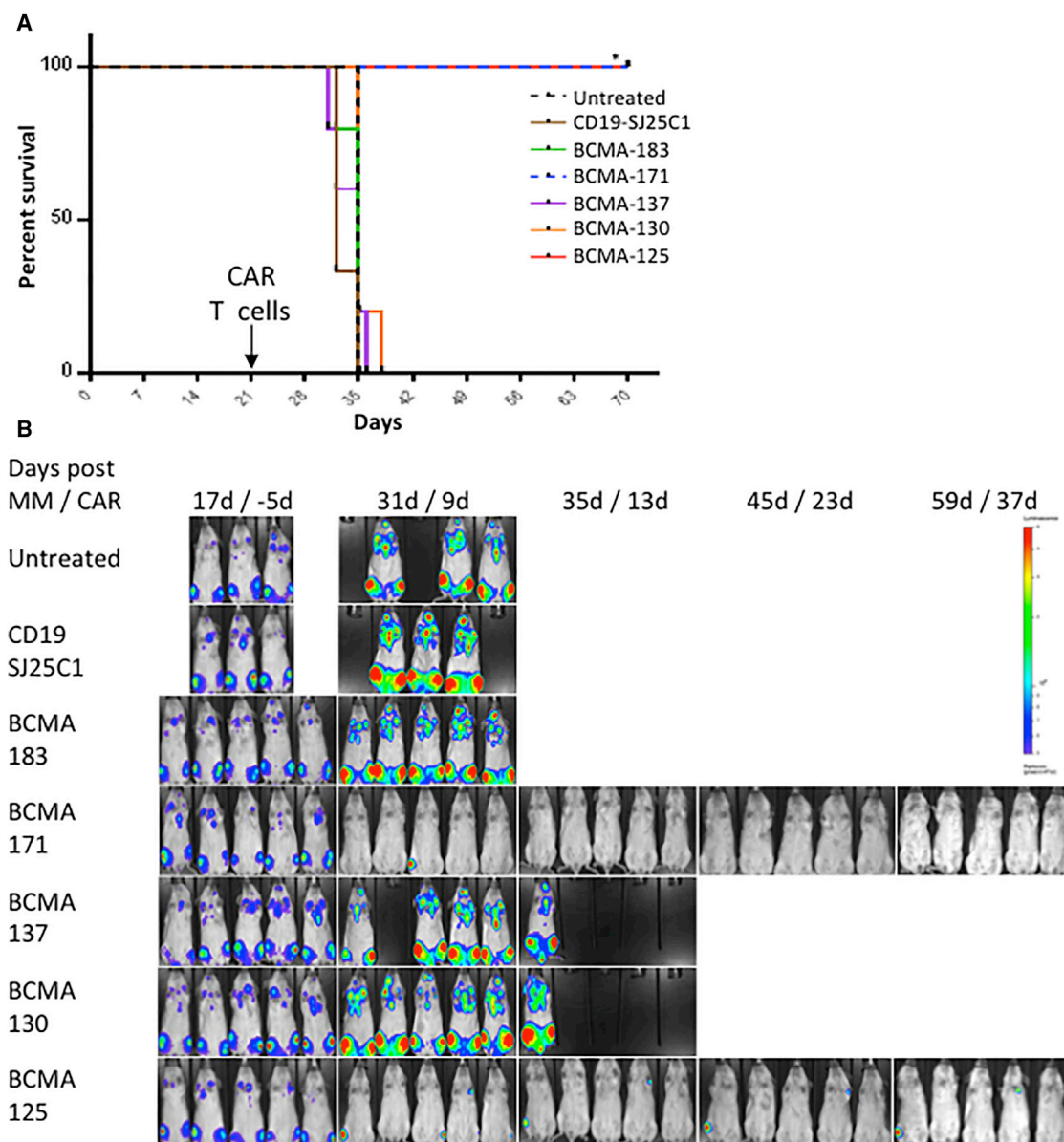


Figure 2. BCMA(171) and BCMA(125) CAR T Cells Prolong Survival and Eradicate Tumors in a High Tumor Burden Xenograft Model of MM

The human bone marrow tropic MM cell line OPM2-fluc was injected via tail vein into NSG mice (1×10^6 OPM2 cells) and allowed to engraft and expand for 21 days. Mice were imaged via bioluminescence (BLI); those with uniform high tumor burden were randomized to either no treatment or treatment with (3×10^6 CAR⁺) gene-modified donor T cells expressing the same CD28-containing CARs as in Figure 1 targeting either CD19(SJ25C1) or BCMA via one of five different human scFvs. (A) Long-term survival was demonstrated specifically in all mice treated with a single dose of BCMA-targeted CAR T cells incorporating either scFv 171 or 125. (B) BCMA-targeted CAR T cells incorporating scFvs 171 and 125 uniquely eradicated high burden of MM as determined by BLI. ($p < 0.001$). BLI of mouse pretreatment (day 17) displayed at a different scale than other time points.

automated flow cytometry cell-cell conjugation assay was developed in which a cell population expressing the query molecule (i.e., anti-BCMA scFv) is mixed with cells expressing a library of cell-surface molecules to identify potential query:target interactions. This approach has the advantage of allowing both the query and library component targets to be presented in the context of the mammalian

plasma membrane, with close to native post-translational modifications and interactions. To this end, we transiently expressed our panel of anti-BCMA scFvs in HEK293 using cell-surface display constructs that contain a cytoplasmic mCherry proximal to the transmembrane domain from murine PD-L1. Simultaneously, we transiently expressed a library consisting of 395 TNFRSF and immunoglobulin

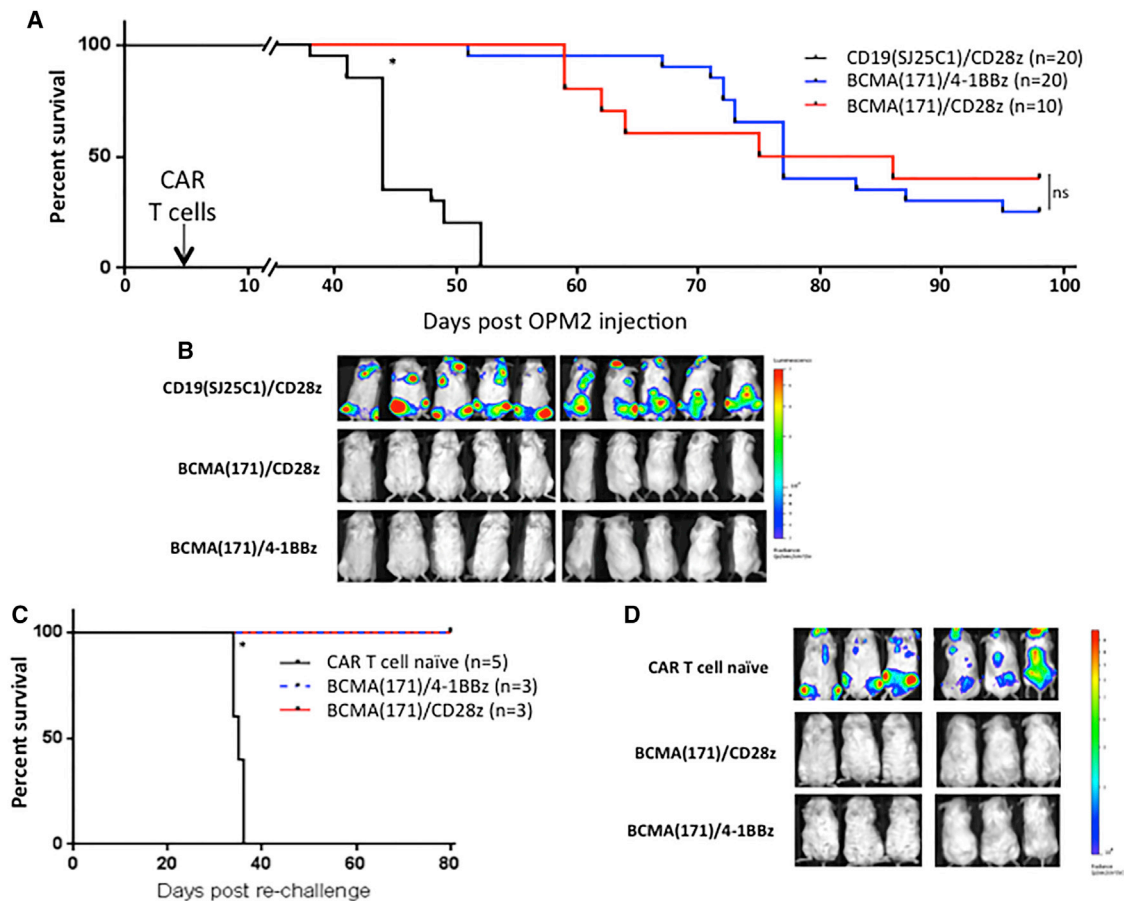


Figure 3. BCMA(171)-Targeted CAR T Cells Provide Long-Term Immunity against Re-challenge with a Human MM Cell Line Irrespective of CAR Co-stimulatory Domain

OPM2-fluc cells (1×10^6) were injected via tail vein into NSG mice. On day 4, mice were treated with a single injection of either control CD19(SJ25C1)- or BCMA(171)-targeted CAR T cells containing a CD28 or a 4-1BB co-stimulatory domain (1×10^6 CAR⁺). (A) Treatment with BCMA(171) CAR T cells provide significantly prolonged survival compared to treatment with CD19(SJ25C1) CAR T cells. Survival between mice treated with BCMA(171) CAR T cells differing by co-stimulatory domain were not significant. (B) Representative ventral and dorsal BLI at day 21 shows elimination of OPM2 MM cells by both groups of BCMA(171) CAR T cells. (C) Long-term surviving mice from 4a were re-challenged with OPM2 cells 98 days after their initial OPM2 injection (94 days after CAR T cell injection). Control CAR T cell naïve mice were simultaneously injected with OPM2 cells. Mice were not re-treated with CAR T cells. BCMA(171) CAR T cell previously treated long-term surviving mice were protected from OPM2 re-challenge and continued to have long-term survival. (D) Imaging from day 34 post-OPM2 re-challenge (day 130 overall) shows substantial MM burden in the CAR T cell naïve injected mice and no OPM2 BLI signal in the previously treated mice ($p < 0.001$).

superfamily members expressed as C-terminal GFP fusions. This library consists only of targets prescreened for both high protein expression and correct membrane localization and represents a diverse set of functionally important immune targets. Mixed scFv query and library cell populations were analyzed by flow cytometry to identify double-positive GFP:mCherry events, representing scFv-target-mediated cell-cell interaction. Of our panel of scFvs, scFv 130 exhibited an off-target interaction with two different isoforms of signal-regulatory protein (SIRP) beta-1 (Figure S2A), while no other screened scFvs, including 171 (Figure 5) demonstrated off-target non-BCMA interactions. We further evaluated the potential for non-specific binding of our lead scFvs via co-culture assay of CAR T cells with isolated primary cells from a variety of essential

normal tissue types. Using interferon gamma (IFN- γ) release as a surrogate for CAR engagement through the scFv, we found IFN- γ release only in the context of CAR T cells co-cultured with positive control human MM cell lines with a signal:noise ratio of $>10,000:1$ (Figure S2B).

Generation of Bicistronic CAR Vector, Including EGFRt, for Clinical Translation

Truncated epidermal growth factor receptor (EGFRt) has been previously developed as a selection marker and potential elimination gene^{21,22} in case of refractory clinical toxicity. We generated a bicistronic construct including the human BCMA(171)/4-1BBz CAR separated by a P2A element with EGFRt for clinical translation

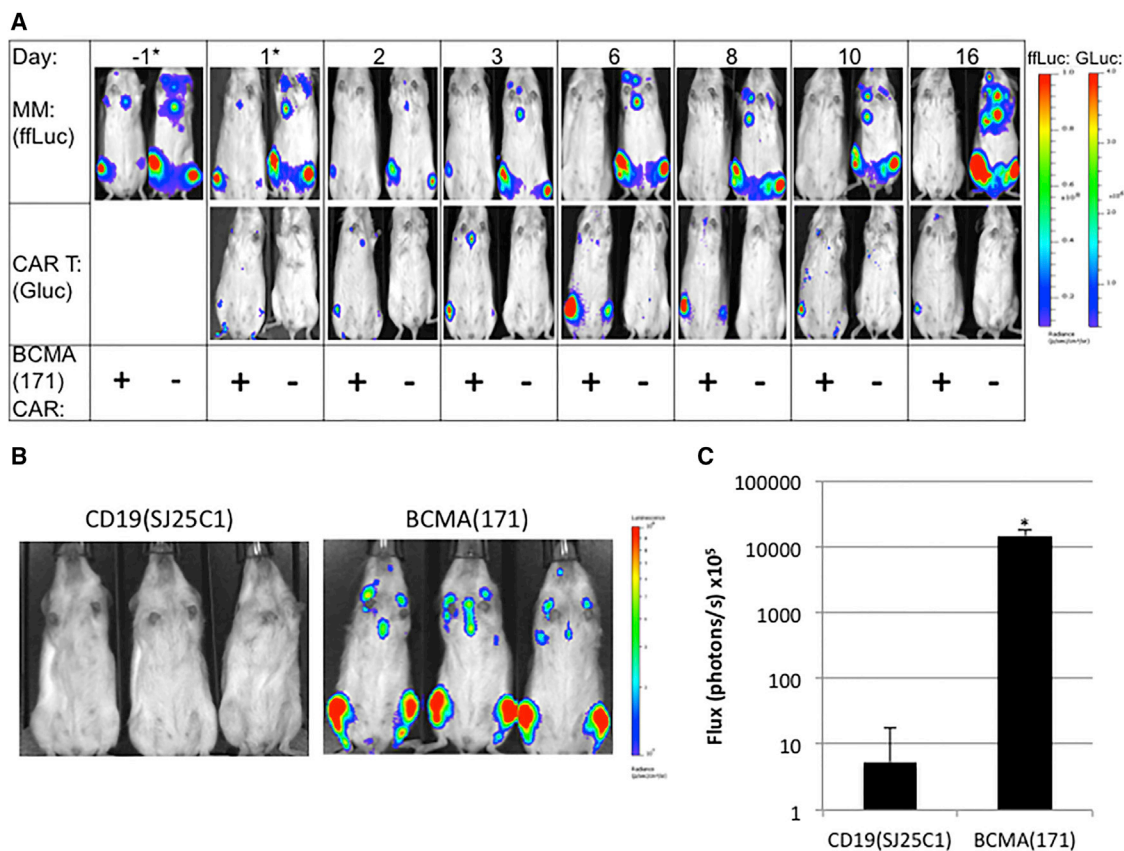


Figure 4. Kinetics of BCMA-Targeted CAR T Cell Accumulation and Tumor Eradication

OPM2-ffLuc cells (1×10^6) were injected via tail vein into NSG mice and allowed to develop high tumor burden for 24 days until treatment with a single dose of human T cells (3×10^6 ; day 0). (A) Mice are treated with either extGLuc/BCMA(171) CAR T (left, +), or untransduced T cells (right, -). A single representative mouse imaged after injection of luciferin (top; OPM2-ffLuc MM cells) and coelenterazine (bottom; extGLuc/BCMA(171)CAR T cells) over time from each group is shown. OPM2-ffLuc bioluminescent signal is eradicated by day 6, corresponding with peak CAR T cell accumulation at site of disease at this time. After clearance of antigen the extGLuc CAR T cell signal contracts over time. (*displayed with a lower BLI scale at these earlier time points). (B) BLI (coelenterazine) on day 6 after treatment with either extGLuc/CD19(SJ25C1) CAR T cells or extGLuc/BCMA(171) CAR T cells. (C) Quantification of the mean coelenterazine mediated BLI signal on day 6 after CAR T cell treatment from the hind limbs of mice in (B) ($n = 6$). Log scale. \pm SEM. (* $p < 0.0001$).

(Figure 5A). Co-expression of the CAR and EGFRt was validated by flow cytometric analysis (Figure 5B). The ability of the EGFR antibody, cetuximab, to facilitate antibody-dependent cellular cytotoxicity (ADCC) of CAR T cells was demonstrated by co-culture of CAR T cells with the natural killer cell line NK-92 (CD16a⁺) in the presence of cetuximab or rituximab, as previously described.²³ EGFRt-expressing CAR T cells, co-cultured with NK-92 cells in the presence of cetuximab, specifically induced ADCC (Figure 5C).

DISCUSSION

Patients with relapsed or refractory MM rarely obtain durable remissions with available therapies. Early clinical use of murine scFv containing BCMA-targeted CAR T cell therapy for advanced MM appears promising.¹⁰ However, murine scFv containing CARs can elicit host immune responses, as was reported with some CD19-targeted CAR T cell therapies for NHL, where anti-murine cellular immunity limited CAR T cell expansion and efficacy of a second

dose of CAR T cells in several patients.⁷ To mitigate the possibility of patient anti-CAR immune responses, herein, we report the development of the first human BCMA-targeted CAR T cell vector.

We screened a human B cell-derived scFv phage display library to identify multiple BCMA-specific human scFvs. An scFv phage display library is particularly beneficial for CAR development, as scFvs can be directly and rapidly cloned into CAR vectors for further evaluation. After our successful screening campaign, we set out to differentiate between multiple human BCMA-targeted scFvs and identify a highly active CAR construct.

Expansion after multiple rounds of antigen stimulation effectively differentiated between CARs incorporating different scFvs (Figure 1B). Given the correlation reported in several trials between CAR T cell expansion in patients and clinical efficacy,^{1,10} as well as the ability of effective CAR T cell therapies to lyse high disease burden

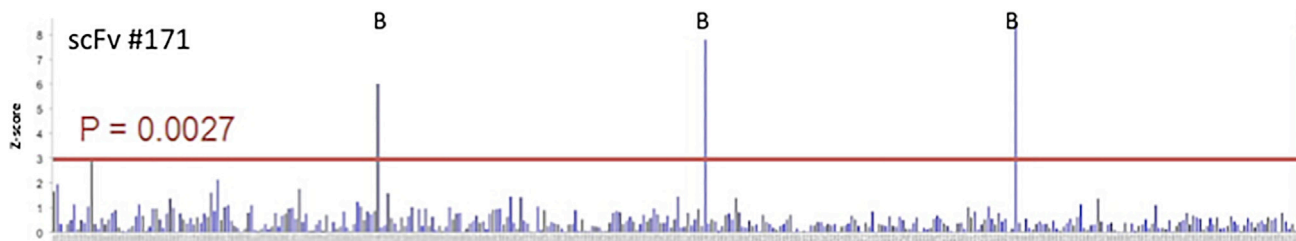


Figure 5. Specificity of BCMA(171)

Vectors containing either (1) BCMA-targeting scFvs with C-terminal mCherry or (2) TNFR and immunoglobulin (Ig) superfamily members with C-terminal GFP were transiently transfected into different populations of HEK293s cells. Potential scFv/target antigen interaction was identified as a double-positive signal by automated flow cytometry. Peaks labeled “B” indicate interactions with BCMA⁺ controls. Unlike scFv clone 130, which interacted with two isoforms of SIRP-B1 (Figure S2A), all other scFvs, including clone 171 (shown), interacted only with BCMA.

in vivo, we hypothesized that an assay characterizing CAR-modified T cells’ ability to maintain high levels of activity over time after multiple stimulation events would mirror the efficacy results of an *in vivo* assay. In this study, we found that the *in vitro* results from this assay predicted the results of more time and resource consuming *in vivo* survival and tumor eradication screening (Figure 2). Thus, expansion after repeat antigen stimulation may decrease the number of CARs that must be evaluated *in vivo* to select a lead candidate for potential clinical translation.

Given the utility of a repeat antigen stimulation assay predicting the differential efficacy of CAR T cell therapies in preclinical *in vivo* studies; we hypothesize that a similar assay may be useful correlative science to clinical trials. In broad terms, lack of efficacy to CAR T cell therapy is caused either by loss of target antigen or lack of functional CAR T cell persistence. While there has been intense focus on monitoring for antigen escape; further study of clinical CAR T cell products may show that the potential for functional persistence could be correlated with the results of such an assay.

We continue to explore the underlying biophysical differences between CAR constructs containing different scFvs that appear to impart different properties they convey to transduced T cells when incorporated into a CAR. ScFvs have similar single-digit nanomolar affinity (Table S1). With the exception of scFv 130, all have similar specificity for BCMA (Figures 5 and S2A). Unlike targets such as CD22 and others where differences in the bound epitope’s proximity to the cell membrane led to apparent differential efficacy of CAR T cells *in vivo*,¹⁶ BCMA has a small (54-amino-acid) extracellular domain; thus, differences in efficacy caused by differential epitope proximity to the membrane are unlikely. We postulate that another characteristic of scFv/antigen interaction may be responsible, and additional potentially differentiating scFv characteristics are the subject of ongoing investigation.

As all factors important for generating an ideal scFv for CAR T cell therapy are not entirely understood, it is beneficial to screen multiple scFvs when generating CARs for potential clinical use. T cells transduced with CARs incorporating the lead scFvs we identified after

in vitro screening eradicated high-volume MM (Figure 2), conveyed durable protection (Figure 3), and demonstrated robust *in vivo* expansion and accumulation at the site of MM (Figure 4). EGFRt/BCMA(171)-41BBz (Figure 6) CAR T cells are under clinical evaluation in a phase I trial that allows for repeat dosing and will be monitored for immune responses to the CAR (NCT03070327). Additional anti-BCMA CAR T cell vectors stemming from this work have entered two separate clinical trials, NCT03338972 and NCT03430011, a phase I/II multi-institutional study.

MATERIALS AND METHODS

Cell Lines and Donor T Cells

The human MM cell line OPM2 was obtained from Deutsche Sammlung von Mikroorganismen und Zellkulturen (DSMZ) and maintained in RPMI and 10% fetal bovine serum (FBS) (Gibco, Life Technologies, Gaithersburg, MD). OPM2 cells were authenticated by STR DNA Profiling (Genetica, Burlington, NC). Human T cells were obtained from either the peripheral blood of healthy donors (MSK IRB#95-054) or from buffy coats prepared from whole blood collected by the New York Blood Center (New York, NY). HEK293GP-GALV9 retroviral packaging cells have been previously described.²⁴

Flow Cytometry

A 10-color Gallios B43618 (Beckman Coulter, Indianapolis, IN) was used to acquire data. Analysis was performed with FlowJo software (V10, Tree Star, Ashland, OR). Expression of CAR was determined by surface staining using either BCMA ECD-Fc (Eureka Therapeutics, Emeryville, CA) or 19E3 (anti-ideotype to SJ25C1 anti-CD19 scFv; MSKCC monoclonal antibody core facility). Cetuximab (Eli Lilly, Indianapolis, IN) and rituximab (Genentech, San Francisco, CA) were obtained from the MSKCC research pharmacy. Cell surface Gaussia luciferase was detected by mouse antisera (#401M, Nanolight, Pinetop, AZ). BCMA-Fc, 19E3, cetuximab, rituximab, and 401M were all conjugated with lightning link labeling kits (Innova Biosciences, Cambridge, UK). Viability is determined by DAPI exclusion (Thermo Fisher, Waltham, MA). Cells are counted with 123count eBeads (Thermo Fisher, Waltham, MA).

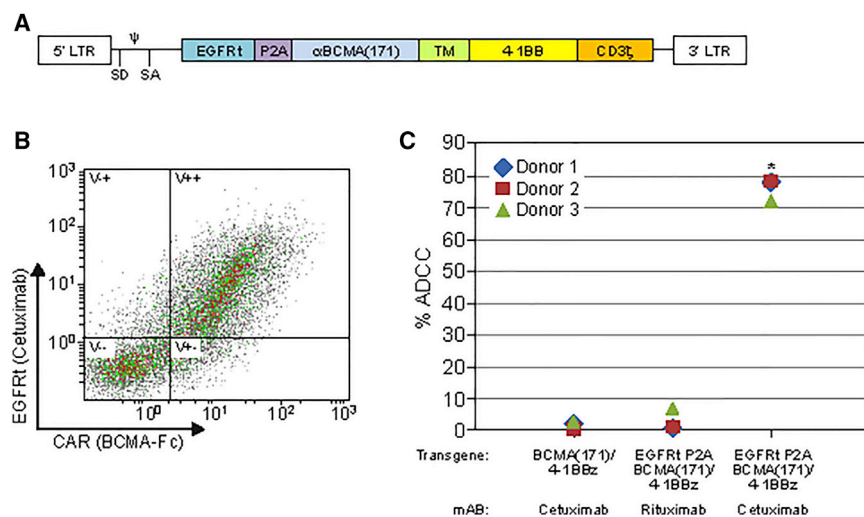


Figure 6. Generation and Validation of EGFRt/BCMA(171)-41BBz Containing CAR T Cell Therapy

(A) Bicistronic vector containing EGFRt and BCMA(171)/4-1BBz separated by a P2A element engineered for clinical translation. (B) FACS shows both the EGFRt and the CAR are co-expressed on transduced donor T cells (quadrant V++). (C) Validation of the potential elimination function of EGFRt was evaluated via co-culture of CAR T cells with CD16⁺ NK-92 cells, in the presence or absence of the EGFRt-specific antibody, cetuximab. Only when both EGFRt was included in the transgene and cetuximab was present in the co-culture was there significant ADCC of CAR⁺ T cells. Pooled data from three independent donors (**p* < 0.005). TNFR, tumor necrosis factor receptor; SF, superfamily; EGFRt, truncated epidermal growth factor receptor; ADCC, antibody-dependent cell-mediated cytotoxicity. P2A, “self-cleaving” peptide; TM, CD8a hinge/transmembrane; LTR, long terminal repeat; SD, splice donor; SA, splice acceptor; Ψ, retroviral packaging element.

Phage Display Library Screen

A human B cell-derived scFv phage display library (E-ALPHA, Eureka Therapeutics, Emeryville, CA) was used to pan against the recombinant human BCMA extracellular domain-IgG1 Fc fusion protein; the positive clones were screened out by ELISA. Unique clones were identified by DNA sequencing. The binding specificity of the unique clones was confirmed by FACS using full-length human BCMA expressing NIH 3T3 cells. The top clones were further confirmed to bind to human MM cell lines by FACS.

Retroviral Constructs

All constructs are in an SFG retroviral plasmid.²⁵ The CAR CD19(SJ25C1)/CD28z (19–28z) has been previously described.^{1,26} In 4-1BB-containing constructs, the CD28 TM and signaling domains have been replaced with a CD8a TM and 4-1BB signaling domain. The variable heavy chain/variable light chain (VH/VL) sequences (linked via [G4S]₃ flexible linker) from scFvs identified in our phage display library screen were cloned into CD28z or 4-1BBz second-generation CARs. EGFRt²¹ and extGLuc²⁷ constructs have been previously described. Bicistronic constructs were generated by separating genes with a P2A sequence. All cloning was performed by restriction enzyme digest or Gibson Assembly (New England Biolabs, Cambridge, MA).

Transduction of Human T Cells

Stable generation of 293GP-GLV9 viral packaging cells and transduction of primary human T cells was done as previously reported.²⁶ In brief, on day 0, healthy donor peripheral blood mononuclear cells (PBMCs) were isolated by ficoll density centrifugation. PBMCs were then activated with phytohemagglutinin (2 μg/mL; Sigma; St. Louis, MO) or CD3/CD28 Dynabeads (Thermo Fisher; Waltham, MA) following manufacturer’s instructions in the presence of IL2. On days 2 and 3, T cells were retrovirally transduced by spinoculation with virus containing supernatant from 293GP-GLV9 cells on retro-nectin (Takara Bio; Shiga, Japan)-coated plates. T cells were further

expanded with IL2 in RPMI plus 10% FBS. Transduction efficiency, cell viability, and quantity were determined by FACS on day 7.

Repeat Antigen Stimulation Expansion Assay

On day –1, BCMA- or CD19-3T3 aAPCs were plated in 6-well plates to establish a monolayer. On day 0, T cells were counted, and 1×10^6 viable CAR⁺ T cells were plated on top of the aAPCs in fresh media in the absence of cytokines. On day 3, new aAPC monolayers were plated as in day 0. On day 4, viable CAR T cells were counted, and 1×10^6 CAR⁺ T cells from wells that expanded (have at least this number of cells) were re-plated on a new monolayer as on day 1. Process is repeated for 3–4 repeat stimulations. Fold expansion after each stimulation is calculated as (viable CAR⁺ T cells on day 4)/ 1×10^6 , the amount of CAR T cells plated on day 1 of each stimulation. To normalize for cells discarded with each new stimulation, cumulative fold expansion is determined by $([\text{fold expansion}_n]) \times [\text{fold expansion}_{n+1}] \dots$. Significance determined by two-way ANOVA.

Cytotoxicity

OPM2 human MM cell lines were stably transduced with ffLuc via retrovirus using the same protocol transduction for human T cells, as described above. 20,000 target cells were plated in U-bottom 96-well plates in triplicate with CAR⁺ T cells at indicated effector-to-target (E:T) ratios and incubated for 4 hr. An ATP-dependent assay was performed as previously described.²⁴ Bioluminescence was read on a Spark microplate reader (TECAN; Mannedorf, Switzerland). Significance determined by two-way ANOVA.

In Vivo Studies

Studies were performed in accordance with Memorial Sloan Kettering Institutional Animal Care and Use Committee approved protocol (00-05-065). Eight- to twelve-week-old NSG (NOD.Cg-Prkdc^{scid} Il2rg^{tm1Wjl}/SzJ) mice (Jackson Labs; Bar Harbor, ME) were injected with the bone marrow tropic cell line OPM2-ffLuc, 1×10^6 cells

via tail vein in all experiments.¹⁹ A single dose of 1×10^6 (4- to 7-day treatment) or 3×10^6 (21- to 24-day treatment) human CAR T cells was injected via tail vein at the time indicated in the experiment. *In vivo* imaging was performed after injection of D-luciferin (Millipore-Sigma; Darmstadt, Germany) or coelenterazine (Nanolight; Pinetop, AZ) with an IVIS Spectrum and analyzed with Living Image software (PerkinElmer; Waltham, MA). Statistical significance between Kaplan-Meier curves determined with log-rank (Mantel-Cox) test. Statistical significance of BLI quantification was determined using Student's t test.

ADCC

Healthy donor T cells isolated from peripheral blood were retrovirally transduced as above with the construct indicated. ADCC was measured by using NK-92 cells (NK cell line expressing CD16) as effectors co-cultured with CAR T cells as targets at a ratio of 1:3 with or without cetuximab or rituximab antibody. At 24 hr, the percentage ADCC was determined by flow cytometric analysis of the decrease in CAR T cells in the presence of cetuximab or rituximab compared to in the absence of cetuximab or rituximab, specifically $([1 - (\text{percentage of CAR T cells in presence of antibody (Ab)} / \text{percentage of CAR T cells in absence of Ab})] \times 100) = \% \text{ ADCC}$.²³ Significance determined by Student's t test.

Generation of an Expression-Validated Library of Ig and TNFRSF Targets

A library of 479 combined Ig superfamily and TNFRSF constructs was generated. Ig superfamily full-length extracellular domains were cloned into a vector containing an erythropoietin (EPO) signal peptide and a transmembrane domain of murine PD-L1 with GFP fused on the C-terminal, cytoplasmic side. In addition, full-length native TNFRSF constructs containing full-length native sequence fused to a C-terminal cytoplasmic GFP were also used for screening. HEK293 suspension cells (Invitrogen) were transiently transfected with cloned library targets, and GFP expression was assessed by flow cytometry. Correct localization for library targets were scored manually by imaging on an inverted EVOS fluorescence microscope. Only targets displaying high GFP expression ($>10^3$) and correct membrane localization were used for further analysis, resulting in a library of 395 targets.

High-Throughput Flow Cytometry Cell-Cell Conjugation Screen

Anti-BCMA scFv sequences were cloned into a Clontech N1 mCherry vector upstream of an inserted transmembrane domain (murine PD-L1) with mCherry fused to the C-terminal cytosolic side. These constructs were transiently transfected in HEK293 Freestyle cells (Invitrogen) using polyethylenimine (PEI) at a 4:1 PEI to DNA ratio (2 μg PEI to 0.5 μg plasmid). In parallel, library constructs were also transfected in HEK293 Freestyle cells. Two days post-transfection, cells were diluted to 1×10^6 cells/mL in $1 \times$ Dulbecco's PBS (DPBS; GE Healthcare Hyclone, Stamford, CT) and 0.2% BSA. Binding reactions were setup in 96-well V-bottom plates by mixing equal volumes of challenger (scFv expressing cells) and library-expressing cells. After binding, cell-cell conjugates were analyzed by flow cytometry

using a Hypercyte sample loader coupled to a BD Accuri flow cytometer. The percent bound was calculated as the number of double-positive events (GFP and mCherry) divided by the total number of cells. The top interactions are shown labeled with Z score values, which were calculated independently for each 96-well plate using the relationship $Z \text{ score} = |(X_{\text{ave}} - X) / \text{SD}|$.

SUPPLEMENTAL INFORMATION

Supplemental Information includes Supplemental Materials and Methods, two figures, and one table and can be found with this article online at <https://doi.org/10.1016/j.ymthe.2018.03.016>.

AUTHOR CONTRIBUTIONS

Conceptualization, E.L.S., C.L., R.J.B.; Methodology, E.L.S., S.C.A., Y.X., H.L.; Investigation and Validation, E.L.S., R.M., M.S., I.J.T., T.J.P., S.C.G.-T., H.L., Y.X.; Resources, I.R., X.W., S.C.A., C.L.; Writing – Original Draft, E.L.S.; Writing – Review & Editing, R.J.B., S.C.A., P.W., X.W., I.R.; Project Administration, E.L.S., P.W.; Supervision, R.B.J., E.L.S., I.R., S.C.A., C.L.; Funding Acquisition, E.L.S., S.C.A., R.J.B.

CONFLICTS OF INTEREST

E.L.S., R.J.B., and C.L. have licensed intellectual property with Juno Therapeutics. R.J.B. and I.R. received research funding from Juno Therapeutics. R.J.B. has a consultancy with Juno Therapeutics. R.M. is an employee of Agenus Inc. P.W., H.L., Y.X., and C.L. are employees and have equity in Eureka Therapeutics. I.R. received research funding from Fate Therapeutics.

ACKNOWLEDGMENTS

All MSK investigators acknowledge MSK Cancer Center Support Core Grant P30 CA008748. E.L.S. is a Special Fellow of The Leukemia & Lymphoma Society; he reports additional support for this work from a Technology Development Grant from MSKCC, the Multiple Myeloma Research Foundation, the Lymphoma Research Foundation, the Society of Immunotherapy for Cancer, and the American Society of Hematology. S.C.A. reports support from the NIH (R01 HG008325, R01 CA198095) and the Albert Einstein Cancer Center (P30 CA013330). R.B.J. reports support from the NIH (R01 CA138738-05, P01 CA059350, P01 CA190174-01), The Annual Terry Fox Run for Cancer Research (New York, NY) organized by the Canada Club of New York, Kate's Team, the Carson Family Charitable Trust, the William Lawrence and Blanche Hughes Foundation, the Emerald Foundation, and the Experimental Therapeutics Center of Memorial Sloan Kettering Cancer Center.

REFERENCES

1. Park, J.H., Rivière, I., Gonen, M., Wang, X., Sénéchal, B., Curran, K.J., Sauter, C., Wang, Y., Santomasso, B., Mead, E., et al. (2018). Long-term follow-up of CD19 CAR therapy in acute lymphoblastic leukemia. *N. Engl. J. Med.* 378, 449–459.
2. Turtle, C.J., Hanafi, L.-A., Berger, C., Gooley, T.A., Cherian, S., Hudecek, M., Sommermeyer, D., Melville, K., Pender, B., Budiarto, T.M., et al. (2016). CD19 CAR-T cells of defined CD4+:CD8+ composition in adult B cell ALL patients. *J. Clin. Invest.* 126, 2123–2138.

3. Lee, D.W., Kochenderfer, J.N., Stetler-Stevenson, M., Cui, Y.K., Delbrook, C., Feldman, S.A., Fry, T.J., Orentas, R., Sabatino, M., Shah, N.N., et al. (2015). T cells expressing CD19 chimeric antigen receptors for acute lymphoblastic leukaemia in children and young adults: a phase 1 dose-escalation trial. *Lancet* 385, 517–528.
4. Maude, S.L., Laetsch, T.W., Buechner, J., Rives, S., Boyer, M., Bittencourt, H., Bader, P., Verineris, M.R., Stefanski, H.E., Myers, G.D., et al. (2018). Tisagenlecleucel in children and young adults with B-Cell lymphoblastic leukemia. *N. Engl. J. Med.* 378, 439–448.
5. Neelapu, S.S., Locke, F.L., Bartlett, N.L., Lekakis, L.J., Miklos, D.B., Jacobson, C.A., Braunschweig, I., Oluwole, O.O., Siddiqi, T., Lin, Y., et al. (2017). Axicabtagene ciloleucel CAR T-cell therapy in refractory large B-cell lymphoma. *N. Engl. J. Med.* 377, 2531–2544.
6. Schuster, S.J., Svoboda, J., Chong, E.A., Nasta, S.D., Mato, A.R., Anak, Ö., Brogdon, J.L., Pruteanu-Malinici, I., Bhoj, V., Landsburg, D., et al. (2017). Chimeric antigen receptor T cells in refractory B-cell lymphomas. *N. Engl. J. Med.* 377, 2545–2554.
7. Turtle, C.J., Hanafi, L.A., Berger, C., Hudecek, M., Pender, B., Robinson, E., Hawkins, R., Chaney, C., Cheria, S., Chen, X., et al. (2016). Immunotherapy of non-Hodgkins lymphoma with a defined ratio of CD8+ and CD4+ CD19-specific chimeric antigen receptor-modified T cells. *Sci. Transl. Med.* 8, 355ra116.
8. Seckinger, A., Delgado, J.A., Moser, S., Moreno, L., Neuber, B., Grab, A., Lipp, S., Merino, J., Prosper, F., Emde, M., et al. (2017). Target expression, generation, preclinical activity, and pharmacokinetics of the BCMA-T cell bispecific antibody EM801 for multiple myeloma treatment. *Cancer Cell* 31, 396–410.
9. Carpenter, R.O., Evbuomwan, M.O., Pittaluga, S., Rose, J.J., Raffeld, M., Yang, S., Gress, R.E., Hakim, F.T., and Kochenderfer, J.N. (2013). B-cell maturation antigen is a promising target for adoptive T-cell therapy of multiple myeloma. *Clin. Cancer Res.* 19, 2048–2060.
10. Ali, S.A., Shi, V., Maric, I., Wang, M., Stroncek, D.F., Rose, J.J., Brudno, J.N., Stetler-Stevenson, M., Feldman, S.A., Hansen, B.G., et al. (2016). T cells expressing an anti-B-cell maturation antigen chimeric antigen receptor cause remissions of multiple myeloma. *Blood* 128, 1688–1700.
11. Tai, Y.-T., Mayes, P.A., Acharya, C., Zhong, M.Y., Cea, M., Cagnetta, A., Craigen, J., Yates, J., Gliddon, L., Fieles, W., et al. (2014). Novel anti-B-cell maturation antigen antibody-drug conjugate (GSK2857916) selectively induces killing of multiple myeloma. *Blood* 123, 3128–3138.
12. Tai, Y.-T., Acharya, C., An, G., Moschetta, M., Zhong, M.Y., Feng, X., Cea, M., Cagnetta, A., Wen, K., van Eenennaam, H., et al. (2016). APRIL and BCMA promote human multiple myeloma growth and immunosuppression in the bone marrow microenvironment. *Blood* 127, 3225–3236.
13. Caruso, H.G., Hurton, L.V., Najjar, A., Rushworth, D., Ang, S., Olivares, S., Mi, T., Switzer, K., Singh, H., Huls, H., et al. (2015). Tuning sensitivity of CAR to EGFR density limits recognition of normal tissue while maintaining potent antitumor activity. *Cancer Res.* 75, 3505–3518.
14. Liu, X., Jiang, S., Fang, C., Yang, S., Olalere, D., Pequignot, E.C., Cogdill, A.P., Li, N., Ramones, M., Granda, B., et al. (2015). Affinity-tuned ErbB2 or EGFR chimeric antigen receptor T cells exhibit an increased therapeutic index against tumors in mice. *Cancer Res.* 75, 3596–3607.
15. Hudecek, M., Lupo-Stanghellini, M.-T., Kosasih, P.L., Sommermeyer, D., Jensen, M.C., Rader, C., and Riddell, S.R. (2013). Receptor affinity and extracellular domain modifications affect tumor recognition by ROR1-specific chimeric antigen receptor T cells. *Clin. Cancer Res.* 19, 3153–3164.
16. Haso, W., Lee, D.W., Shah, N.N., Stetler-Stevenson, M., Yuan, C.M., Pastan, I.H., Dimitrov, D.S., Morgan, R.A., FitzGerald, D.J., Barrett, D.M., et al. (2013). Anti-CD22-chimeric antigen receptors targeting B-cell precursor acute lymphoblastic leukemia. *Blood* 121, 1165–1174.
17. Lamers, C.H.J., Willemsen, R., van Elzakker, P., van Steenberg-Langeveld, S., Broertjes, M., Oosterwijk-Wakka, J., Oosterwijk, E., Sleijfer, S., Debets, R., and Gratama, J.W. (2011). Immune responses to transgene and retroviral vector in patients treated with ex vivo-engineered T cells. *Blood* 117, 72–82.
18. Karimi, M.A., Lee, E., Bachmann, M.H., Salicioni, A.M., Behrens, E.M., Kambayashi, T., and Baldwin, C.L. (2014). Measuring cytotoxicity by bioluminescence imaging outperforms the standard chromium-51 release assay. *PLoS One* 9, e89357.
19. Lawson, M.A., Paton-Hough, J.M., Evans, H.R., Walker, R.E., Harris, W., Ratnabalan, D., Snowden, J.A., and Chantry, A.D. (2015). NOD/SCID-GAMMA mice are an ideal strain to assess the efficacy of therapeutic agents used in the treatment of myeloma bone disease. *PLoS One* 10, e0119546.
20. Ghosh, A., Smith, M., James, S.E., Davila, M.L., Velardi, E., Argyropoulos, K.V., Gunset, G., Perna, F., Kreines, F.M., Levy, E.R., et al. (2017). Donor CD19 CAR T cells exert potent graft-versus-lymphoma activity with diminished graft-versus-host activity. *Nat. Med.* 23, 242–249.
21. Wang, X., Chang, W.-C., Wong, C.W., Colcher, D., Sherman, M., Ostberg, J.R., Forman, S.J., Riddell, S.R., and Jensen, M.C. (2011). A transgene-encoded cell surface polypeptide for selection, in vivo tracking, and ablation of engineered cells. *Blood* 118, 1255–1263.
22. Paszkiewicz, P.J., Fräßle, S.P., Srivastava, S., Sommermeyer, D., Hudecek, M., Drexler, I., Sadelain, M., Liu, L., Jensen, M.C., Riddell, S.R., and Busch, D.H. (2016). Targeted antibody-mediated depletion of murine CD19 CAR T cells permanently reverses B cell aplasia. *J. Clin. Invest.* 126, 4262–4272.
23. Yamashita, M., Kitano, S., Aikawa, H., Kuchiba, A., Hayashi, M., Yamamoto, N., Tamura, K., and Hamada, A. (2016). A novel method for evaluating antibody-dependent cell-mediated cytotoxicity by flow cytometry using cryopreserved human peripheral blood mononuclear cells. *Sci. Rep.* 6, 19772.
24. Laurent, S.A., Hoffmann, F.S., Kuhn, P.-H., Cheng, Q., Chu, Y., Schmidt-Suppran, M., Hauck, S.M., Schuh, E., Krumbholz, M., Rübsamen, H., et al. (2015). γ -Secretase directly sheds the survival receptor BCMA from plasma cells. *Nat. Commun.* 6, 7333.
25. Rivière, I., Brose, K., and Mulligan, R.C. (1995). Effects of retroviral vector design on expression of human adenosine deaminase in murine bone marrow transplant recipients engrafted with genetically modified cells. *Proc. Natl. Acad. Sci. USA* 92, 6733–6737.
26. Quintás-Cardama, A., Yeh, R.K., Hollyman, D., Stefanski, J., Taylor, C., Nikhamin, Y., Imperato, G., Sadelain, M., Rivière, I., and Brentjens, R.J. (2007). Multifactorial optimization of gammaretroviral gene transfer into human T lymphocytes for clinical application. *Hum. Gene Ther.* 18, 1253–1260.
27. Santos, E.B., Yeh, R., Lee, J., Nikhamin, Y., Punzalan, B., Punzalan, B., La Perle, K., Larson, S.M., Sadelain, M., and Brentjens, R.J. (2009). Sensitive in vivo imaging of T cells using a membrane-bound Gaussia princeps luciferase. *Nat. Med.* 15, 338–344.